

Chapter 1

1.1 Introduction

The demand for multifunctional and miniaturized products has increased in recent years, and related research is still in progress. *Multifunctional materials* have dawned huge interest due to their physical properties such as magnetic, electrical, optical, elastic, etc. These physical properties strongly depend on the synthesis, microstructure, and electronic structure and make them useful for various applications in information and technology, digital data storage, computer technology, etc.

Multiferroic ceramics are materials in which different physical properties are combined in a single material. In latest years, multiferroic materials have become one of the freshest research ideas and roused abundant reviews in the last few years [Eerenstein *et al.* 2006; Cheong *et al.* 2007; Schmid *et al.* 2008; Khomskii *et al.* 2009; Wang *et al.* 2010; Ma *et al.* 2011; Pantel *et al.* 2012; Scott *et al.* 2013; Park *et al.* 2014; Ren *et al.* 2015; Fiebig *et al.* 2016; Yin *et al.* 2017]. These materials have potential applications that could be used in multi-state memory elements (sensors) and multi-mode devices (spintronics) [Spaldin *et al.* 2017]. Other applications of multiferroics are used in transducer, actuators, aerospace, microelectronics, laser technology, microwave, electrical/radio technology, telecommunications, computing, defense, electro-optical modulator, light valves, *etc.* applications [Choudhary *et al.* 2008].

Most of the investigated multiferroic materials are oxides, predominantly Bi-based perovskites, and hexagonal manganites. BiFeO_3 is the most explored compound among all the multiferroic substances as it is a strongly correlated oxide system [Ahn *et al.* 2003; Dagotto *et al.* 2005]. It offers a pathway to realize novel electronic devices in which

superconductivity [Bednorz *et al.* 1988], magnetism, and metal-insulator transitions [Imada *et al.* 1998] can be controlled by using an external electric field. This system also includes phenomena, *e.g.*, high-temperature colossal magneto resistant (CMR) materials [Imada *et al.* 1998], heterostructures with 2D electron gases at epitaxial interfaces [Huijben *et al.* 2006; Thiel *et al.* 2006; Cen *et al.* 2008]. Some basic terms related to structure, properties, and mechanisms are discussed in the following section.

1.2 Structural symmetry

The crystal symmetry of a crystal depends on its lattice structure. The crystal structure could be explained as the basis of the Bravais lattice of the crystal. All the crystals are divided into 32-point groups, as shown in Fig. 1.1. A point group has eight symmetry elements (excluding translation symmetry), and their rotation axis are as follows: 1 (without rotation), 2 (rotation diad), 3 (rotation triad), 4 (rotation tetrad), 6 (rotation hexad), $\bar{4}$ (rotation-inversion tetrad axis), inversion center i and reflection mirror m [Fjellvåg 1994]. Structural symmetry affects both physical and structural properties of crystals, such as ferroelectric, dielectric, piezoelectric, nonlinear optical properties, and elasticity. Out of 32-point groups, 11 are centrosymmetric, *i.e.*, $\bar{1}$, $2/m$, mmm , $(4/m)mm$, $4/m\bar{m}$, $\bar{3}$, $\bar{3}m$, $6/m$, $(6/m)mm$, $m\bar{3}$, $m\bar{3}m$. The crystal's symmetric center doesn't possess any polarity. 21-point groups are non-centrosymmetric. They are as follows: 1, 2, 222, 4, 32, 6, 622, 23, 3, m , $mm2$, $\bar{4}$, $\bar{4}2m$, $4mm$, $3m$, $\bar{6}2m$, $6mm$, $\bar{6}$, $\bar{4}3m$, 432 [Xu 1991]. These crystals possess one or more unique direction axes. These point groups exhibit piezoelectricity except 432. 10-point groups have a single unique directional axis. They are as follows: 1, 2, m , $mm2$, 4, $4mm$, 3, $3m$, 6, $6mm$ [Xu 1991, Fjellvåg 1994].

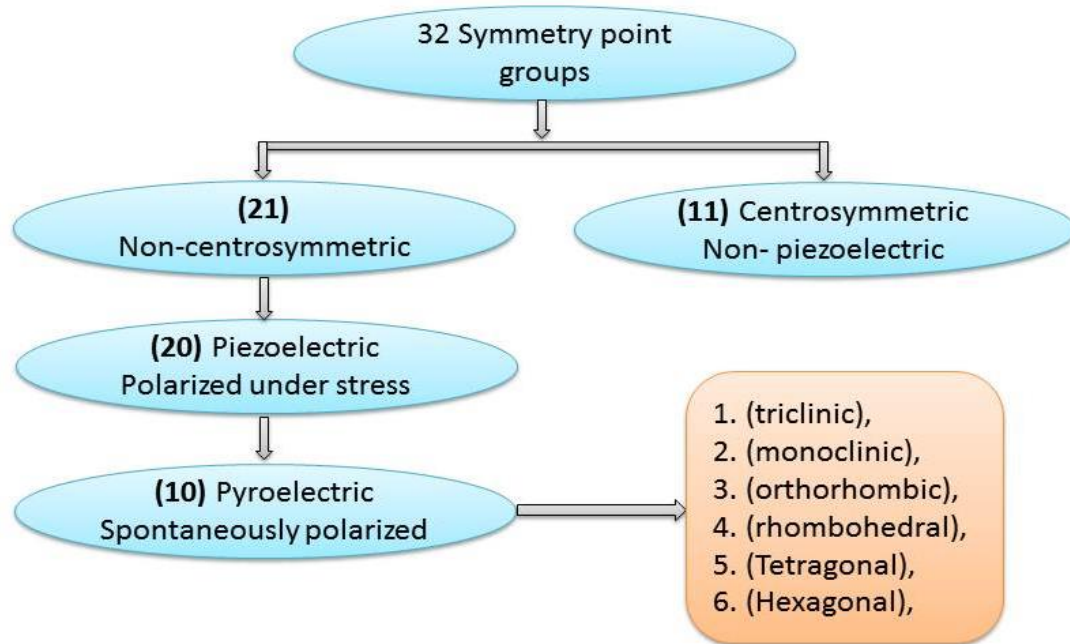


Fig. 1.1: Classification of crystal classes.

1.2.1 Ferroic materials

Ferroic materials are functional materials having symmetry, and the physical properties are affected by the environmental conditions that are influenced by changing temperature, pressure, electric and magnetic fields. There are four types of ferroic orders: ferromagnetism, ferroelectric, ferroelastic, and ferrotoroidics. These ferroic orders are encapsulated in semiconducting or insulating materials having permanent dipoles [Cullity *et al.* 2011]. The ferroic materials are mainly used in sensors, actuators, and memory storage devices due to their large non-linear coefficient and spontaneous order parameters. Ferroic materials also show a phase transition from non-ferroic to ferroic at a specific temperature. The ferroic materials exhibit a hysteresis loop when a spontaneous magnetic, electrical or mechanical field is applied, as shown in Fig.1.2.

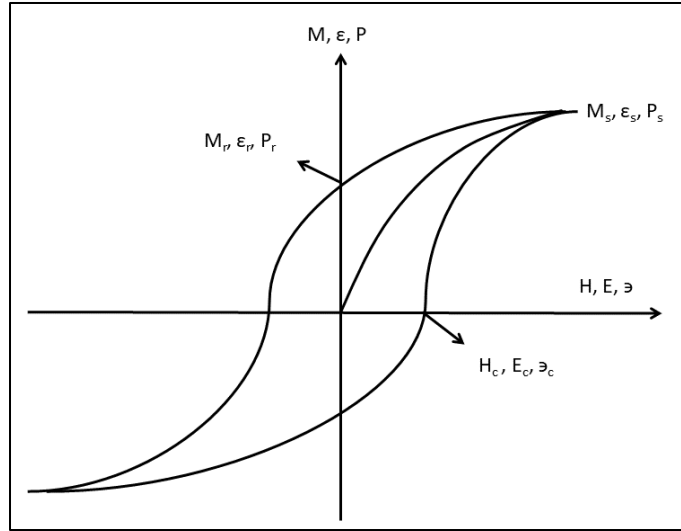


Fig. 1.2: Hysteresis loop for ferroic materials.

The spontaneous order parameters (M , P , ϵ) in the materials don't reveal until they are exposed to any external forces [strain (ϵ), electric field (E), and magnetic field (M)] because of the formation of small volumes (domains). These domains are so arranged that their net ordered moment is canceled out. On applying field, the domains are started aligning themselves in the direction of the field. The order parameters are increased to a certain value and then saturated (M_s , P_s , ϵ_s). When the field is decreased to zero, the order parameters do not retrace the path and reach (M_r , P_r , ϵ_r). When the field is reversed, the net order parameters become zero at a specific field called coercivity (M_c , P_c , ϵ_c) and ϵ - ϵ , P - E , and M - H the response is hysteric [Cullity *et al.* 2011].

1.2.2 Ferroelectrics

Ferroelectrics are the polar dielectric materials with spontaneous electric polarization in a specific temperature range known as *Curie temperature* (T_c), which could be reversed by applying the external electric field. The phenomenon is known as ferroelectricity [Xu 1991]. The crystal below T_c undergoes paraelectric to a ferroelectric phase transition. Ferroelectrics could possess net dipole moment in the absence of an electric field. The phase transition in

ferroelectrics causes strong incongruities in the physical properties such as dielectric, elastic, and thermal, so the symmetry of the paraelectric phase is always higher than the ferroelectric phase. Ferroelectrics are used in memory storage devices, sensors, and vibrators. Rochelle salt ($\text{NaKC}_4\text{H}_4\text{O}_6 \cdot 4\text{H}_2\text{O}$) is the first ferroelectric material discovered in 1920. Naturally, ferroelectrics have a multi-domain state; applying an electric field reduces the domain (ceramics) or disappears (crystals). In ferroelectrics, domain wall switching results in the hysteresis loop, as shown in Fig. 1.1. In an antiferroelectric, net spontaneous polarization becomes zero due to ferroic entities are spontaneously polarized in anti-parallel direction (Kittel *et al.* 1951). On the basis of crystal structure and chemical composition, ferroelectrics are divided into four categories [Lines *et al.* 2004]:

- (a) Tartarate group: *e.g.*, Rochelle salt ($\text{NaKC}_4\text{H}_4\text{O}_6 \cdot 4\text{H}_2\text{O}$)
- (b) KDP (KH_2PO_4) and TGS (Triglycine sulphate)
- (c) Oxygen octahedral group:
 - (i) The ferroelectric perovskite-type
 - (ii) Antiferroelectric and cell-doubling Perovskite-type
 - (iii) Lithium tantalate and Lithium niobate
 - (iv) Tungsten-bronze type
 - (v) Pyroclore-type ferroelectrics
- (d) Ganidine aluminium hexahydrate $\text{NHC}(\text{NH}_2)_2\text{AlH}(\text{SO}_4)_2 \cdot 10\text{H}_2\text{O}$

1.2.2.1 Perovskite ferroelectrics

Perovskite was discovered by “Gustav Rose” in 1839 and named after a Russian mineralogist “Lev Perovski” [Orlovskaya *et al.* 2003]. Among all the ferroelectric materials, perovskites are extensively studied. Perovskites possess a cubic structure narrowly with the

general formula ABO_3 , where A is cations (bigger) and located at the corner of the cube. These are generally rare-earth or alkaline earth elements; B is a (smaller) cation located at the center of the lattice; these are generally $3d$, $4d$, and $5d$ transition metal elements. The stability (rotation, tilting, and distortion of the octahedra) of perovskite compounds is determined by the tolerance factor (t). The tolerance factor should exist within the range of 0.75-1.0 [Peña *et al.* 2001]. Tolerance factor is defined as:

$$t = \frac{R_A + R_O}{\sqrt{2}(R_B + R_O)} \quad (1.1)$$

Where R_A , and R_B are ionic radii of cations at A and B sites, while R_O is the ionic radius of oxygen. Fig. 1.3 shows a typical perovskite structure. In the perovskite structure A-O bond is coordinated by coordination number 12; B-O is coordinated by coordination number 6, while O is coordinated with B by coordination number 2. A-O bond is 40% larger than the B-O bond [Verma *et al.* 2009].

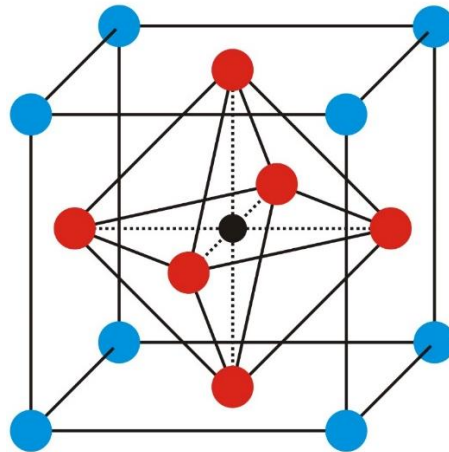


Fig. 1.3: The perovskite structure [Orlovskaya *et al.* 2003].

The rigidity of the oxygen octahedra network causes the lattice constant of the primary perovskite unit cell to nearly 4 \AA . The ionic radius of oxygen is approximately 1.40 \AA (CN=6) [Orlovskaya *et al.* 2003]. The primary cubic structure of perovskites gets distorted

due to the occupancy of cations of different sizes at A and B sites along (a) the [100] direction, which results in a tetragonal cell, (b) the [110] direction leads to an orthorhombic cell, (c) the [111] direction, leads to a rhombohedral cell, or (d) arbitrary [hkl] directions, producing monoclinic and triclinic cell [Megaw *et al.* 1952, Glazer *et al.* 1975]. Seemingly, only the distorted structures, which are non-centrosymmetric, are ferroelectric.

1.2.3 Magnetism

Magnetism is the physical property of some materials that get attracted or repelled by the magnetic field. Lodestone (Fe_3O_4) is the first discovered permanent magnet. The magnetic field is caused due to the magnetic moments and electric currents of elementary particles. There are three responsible factors for the magnetic moment in an atom/ion: (i) spin of electrons; (ii) orbital angular momentum of electron about the nucleus; and (iii) change in the orbital moment induced by an applied magnetic field. The first two factors cause magnetic moment in material and provide paramagnetism, and the third one leads to a diamagnetic contribution [Cullity *et al.* 2011]. Depending on the interactions between the magnetic dipoles, the materials exhibit (a) diamagnetism, (b) paramagnetism, (c) ferromagnetism, (d) antiferromagnetism, and (e) ferrimagnetism [Callister *et al.* 2018].

1.2.3.1 Ferromagnetism

These materials have parallelly aligned, unpaired electron spins in the same direction in a particular region called domain, as shown in Fig. 1.4 [Cheong *et al.* 2020]. In the domain region, magnetism is very intense. Still, at bulk levels, many domain regions exist which are randomly oriented to each other, and the material remains demagnetized. When an external magnetic field is applied to ferromagnetics, the domains get aligned in the direction of the field. This alignment of domains remains in the material even after the removal of the field

and hence possesses permanent magnetization and has a large positive value of susceptibility. Ferromagnetics shows a nonlinear relationship between the externally applied magnetic field (H) and the magnetization (M), known as the hysteresis curve, as shown in Fig. 1.1. The magnetic hysteresis loop shows the amount of energy loss per cycle of magnetism. On applying a sufficient higher magnetic field to a magnetic material, the loop gets saturated at the saturation magnetization (M_s) point. Further, when the magnetic field is reduced to zero, the material has a remanent magnetization called (M_r). When the magnetic field is reversed, the magnetization is eventually reduced to zero at a point called coercivity (H_c). Ferromagnetics becomes paramagnetic above a specific temperature called Curie temperature (T_C). The susceptibility of ferromagnetic materials is calculated with the Curie-Weiss law given by the formula:

$$\chi = \frac{T}{T-T_C} \tag{1.2}$$

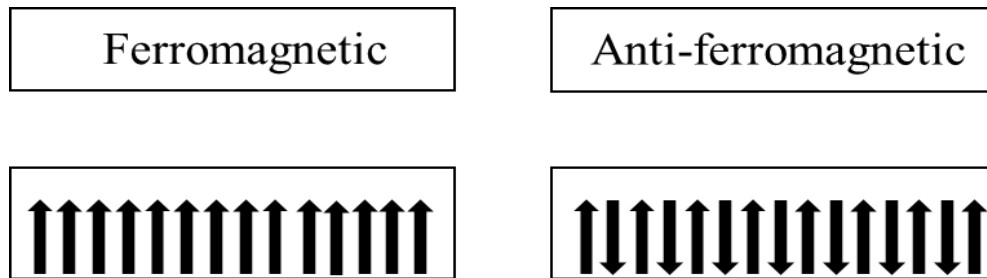


Fig. 1.4: Spin orientations of ferromagnetic and anti-ferromagnetics materials.

1.2.3.2 Antiferromagnetism

These are the materials in which the magnetic moment tends to aligned in anti-parallel order in a domain to the adjacent domains so, the net magnetization tends to zero, as shown in Fig. 1.4. The antiferromagnetism exists below a specific temperature known as Néel temperature (T_N), and above this, these are paramagnetic in nature. At T_N anti-ferromagnetics attain maximum susceptibility. At absolute 0 K, anti-ferromagnetic materials are diamagnetic, but

they could also exhibit ferromagnetism at varying temperatures [Néel 1952]. In a few antiferromagnetic materials, net magnetizations are not zero due to the geometrical arrangement is such that each pair of neighbors are not anti-aligned. This is called a “spin glass” and is an example of “geometrical frustration” [Callister *et al.* 2018].

1.2.3.3 Magnetic ordering

Magnetic ordering is the interaction of magnetic spins, which are arranged, in an ordered pattern within the crystallographic lattice. The Heisenberg model using the Hamiltonian equation defines the interaction between the adjacent spins S_i and S_j :

$$\hat{H} = \sum_{ij} J_{ij} \mathbf{S}_i \cdot \mathbf{S}_j \quad (1.3)$$

Where J_{ij} is an exchange constant that describes the nature of the interaction between \mathbf{S}_i and \mathbf{S}_j . For a ferromagnetic system, J_{ij} is positive, which means adjacent spins are aligned parallel to each other in the same direction. If J_{ij} is negative, adjacent spins are aligned antiparallel to each other that resembles an anti-ferromagnetic system. Based on spin, periodicity in the crystal structure is divided into commensurate or incommensurate. Examples of commensurate antiferromagnetic order are A-type and G-type orders, as shown in Fig. 1.5. Examples of incommensurate antiferromagnetic order are sinusoidally modulated spin density waves and cycloidal order, in which the spins change orientation along the propagation direction inside a circular or ellipsoidal envelope (Fig. 1.6). Anions and cations usually arrange themselves in crystal systems in a manner to minimize the effects of electrostatic repulsion. This arrangement is dependent on the atomic orbitals and influences the magnetic properties. The compounds discussed in this thesis have perovskite crystal structures, with a central Bi^{3+} ion surrounded by an octahedron of O^{2-} ions.

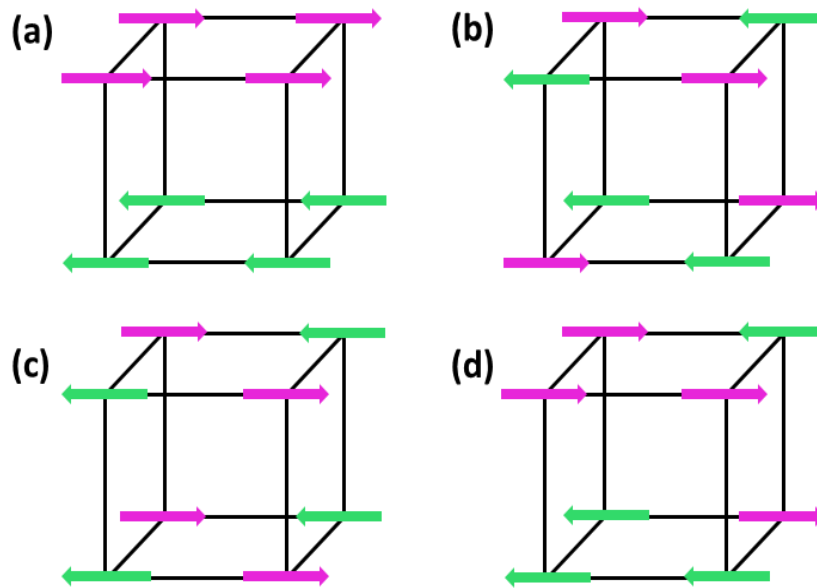


Fig. 1.5: (a) A-type, (b) G-type, (c) C-type and (d) E-type commensurate antiferromagnetic order.

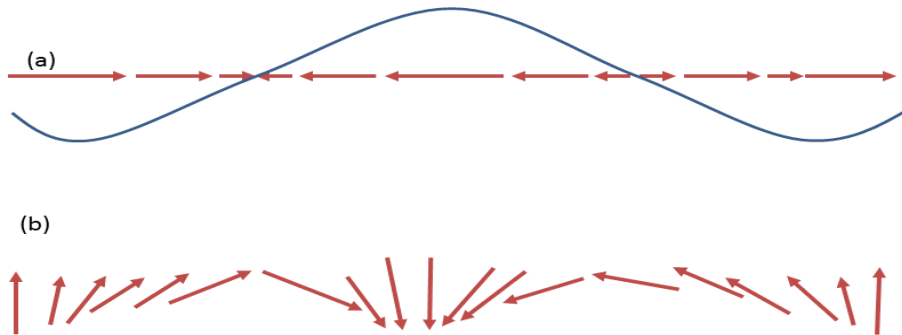


Fig. 1.6: (a) sinusoidal and (b) cycloidal incommensurate antiferromagnetic order.

1.2.3.4 Magnetic interactions

The exchange interaction between magnetic moments causes long-range magnetic ordering. For *direct exchange*, the interaction occurs between the neighboring moments. If the strong interaction (antiferromagnetic coupling) occurs between two next-to-nearest

neighbor cations through a non-magnetic anion, it is termed indirect exchange or superexchange or Kramers–Anderson superexchange. This can be explained by considering a system with two magnetic atoms, individually having a single d -orbital electron, parted by an oxygen atom. In an ionically bonded system, the oxygen ion has two electrons in its p -orbital, which overlaps with the d -orbitals of the magnetic atoms (Fig. 1.7).

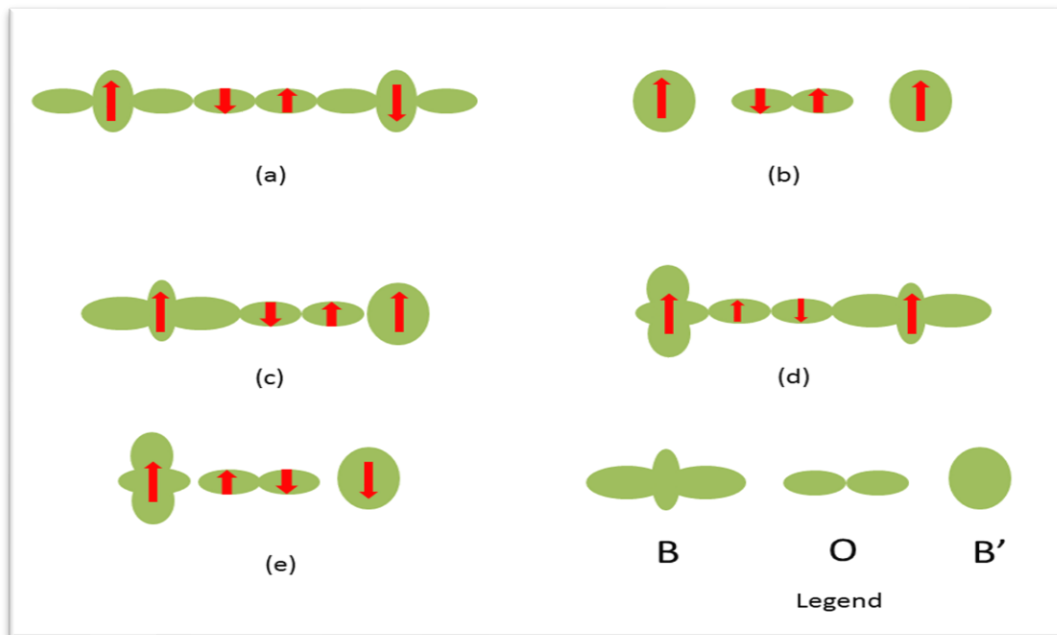


Fig. 1.7: Different magnetic orders of superexchange interaction [Goodenough *et al.* 1961]

On the basis of valence band theory and Pauli exclusion principle, Goodenough–Kanamori rules have explained the magnetic properties of a wide range of materials as:

- (a) If two magnetic ions with half-filled orbitals couple through an intermediary non-magnetic ion (*e.g.*, O^{2-}), the superexchange would be strongly anti-ferromagnetic.

- (b) If the coupling occurs between an ion with a filled orbital and one with a half-filled orbital would be ferromagnetic.
- (c) The coupling between an ion with either a half-filled or filled orbital and one with a vacant orbital can be either antiferromagnetic or ferromagnetic but usually favors ferromagnetic.
- (d) When multiple types of interactions are present concurrently, the antiferromagnetic is leading as it is independent of the intra-atomic exchange term.

1.2.4 The magnetoelectric effect

An intrinsic coupling between electrical and magnetic properties of a material is known as the magnetoelectric effect. Landau's theory framework describes the thermodynamics of coupling between ferromagnetics and ferroelectrics by the expansion of free energy for a magnetoelectric system [Liu 2011, Fiebig 2005].

$$F(E, H) = F_0 - P_i^s E_i - M_i^s H_i - \frac{1}{2} \varepsilon_0 \varepsilon_{ij} E_i E_j - \frac{1}{2} \mu_0 \mu_{ij} H_i H_j - \alpha_{ij} E_i E_j - \frac{1}{2} \beta_{ijk} E_i H_j H_k - \frac{1}{2} \gamma_{ijk} H_i E_j E_k - \frac{1}{4} \delta_{ijkl} H_i H_j E_k E_l - \dots \quad (1.5)$$

where F_0 is the ground state free energy, (i, j, k, l) are the subscripts for those four components of a variable in spatial coordinates, E_i and H_i are the components of the electric E and magnetic field H , P_i^s and M_i^s are the components of spontaneous polarization and magnetization, ε_0 and μ_0 are the dielectric permittivity and magnetic permeability, respectively, in a vacuum, ε_{ij} and μ_{ij} are the second-order tensors of dielectric permittivity and magnetic permeability, α_{ij} are the coefficients of linear ME tensor, β_{ijk} and γ_{ijk} are the third-order tensors describing quadratic coupling, and δ_{ijkl} is the fourth-order tensor expressing biquadratic coupling.

After derivation of the free energy, we can obtain the polarization

$$P_i(E, H) = -\frac{\partial F}{\partial E_i} = P_i^s + \varepsilon_0 \varepsilon_{ij} E_j + \alpha_{ij} H_j + \frac{1}{2} \beta_{ijk} H_j H_k + \gamma_{ijk} H_i E_j + \frac{1}{4} \delta_{ijkl} H_j H_k E_l \quad (1.6)$$

$$M_i(E, H) = -\frac{\partial F}{\partial H_i} = M_i^s + \mu_0 \mu_{ij} H_j + \alpha_{ij} E_j + \beta_{ijk} H_j E_i + \gamma_{ijk} \frac{1}{2} \gamma_{ijk} E_j E_k + \frac{1}{4} \delta_{ijkl} H_j E_k E_l \quad (1.7)$$

A multiferroic that is ferromagnetic and ferroelectric is prone to display higher linear magnetoelectric effects. This is because ferroelectric and ferromagnetic materials possess a large permittivity and permeability, respectively. The linear ME coefficient α_{ij} is limited by the relation.

$$\alpha_{ij}^2 \leq \varepsilon_0 \mu_0 \varepsilon_{ii} \mu_{jj} \quad (1.8)$$

Where ε_{ii} and μ_{jj} are permittivity and magnetic permeability, respectively.

1.3 Multiferroics

W. Röntgen, in 1888, was the first scientist who found that dielectric material moving through an electric field would become magnetized. In 1894 P. Curie speculated the reverse magnetoelectric effect in non-moving materials, *i.e.*, intrinsic ME was considered due to symmetry. L. D. Landau and E. Lifshitz gave the mathematical formulation of the linear magnetoelectric effect; this phenomenon was restricted in time asymmetric media with breaking time-reversal symmetry [Landau *et al.* 1960]. In 1960 Dzyaloshinskii foreboded theoretically, and then Astrov *et al.* 1960 proved practically that antiferromagnetic Cr_2O_3 exhibited a linear ME effect, *i.e.*, electric field-induced magnetization. Later in 1961, Astrov *et al.* experimentally verified that a magnetic field could induce polarization, and Indenbom *et al.* in 1960, determined the tensor form of linear ME coupling coefficient (α_{ij}) with an incomplete list of point groups. There are several textbooks and reviews [Bhagaivantam *et al.* 1966; Birss *et al.* 1966; Siratori *et al.* 1992] with complete tables of point groups that permitted linear ME effect. The largest ME coupling was perceived in LiCoPO_4 [Rivera *et al.* 1993], yttrium iron garnet (YIG) films [Krichevtsov *et al.* 1989], and TbPO_4 [Rado *et al.* 1984], but as seen from the application point of view, these materials were still lag for appropriate properties.

Later it was found that some of the materials were shown cross-coupling between two or more *ferroic* orders like ferroelectrics, ferromagnetics, ferroelastics, and ferrotoroidics, in the absence of an external field at the same temperature. So, for this special class of materials H. Schmid 1994 coined the term multiferroics. The coexistence of ferroic orders has many potential applications, such as “four state memory devices” based on four different types of coupling between polarization and magnetization, which enhance the data storage density.

Nickel iodine boracite ($\text{Ni}_3\text{B}_7\text{O}_{13}\text{I}$) was the first compound in which multiferroicity was observed, but it had complex structures. It did not find much attraction from the technological point of view. Then, the researchers made lots of efforts for different multiferroic compounds, which included rare-earth manganites and ferrites (*e.g.*, TbMnO_3 , HoMn_2O_5 , LuFe_2O_4 , and PZTFT). Other examples were bismuth compounds (BiFeO_3 and BiMnO_3), non-oxides such as BaNiF_4 , and spinel chalcogenides (ZnCr_2Se_4). A solid solution of $\text{Pb}(\text{Fe}_{2/3}\text{W}_{1/3})\text{O}_3$ and $\text{Pb}(\text{Mg}_{1/2}\text{W}_{1/2})\text{O}_3$ was discovered [Smolenskii *et al.* 1959]. Among all multiferroic systems, perovskite transition metal oxides were highly explored. Out of 32, only 13-point groups allow the simultaneous occurrence of two or more ferroic orders due to symmetry because symmetry may not play an important role in determining the multiferroic. But all ferroelectrics and ferromagnetics do not show simultaneous space inversion and time-reversal symmetry, as shown in Fig. 1.8. It shows the behavior of all forms of ferroic order under space and time reversal.

From the microscopic view, the presence of localized electrons is the basis of magnetism in all the magnets. The partially filled shells, *i.e.*, *d*-orbital of transition metals and *f*-orbital of rare earths, have a corresponding localized spin or magnetic moment. The exchange interaction between these localized spins leads to magnetic ordering. But there are many and different ways

for ferroelectricity, so on the basis of ferroelectric ordering, mainly two types of multiferroics are classified as Type-I and Type-II.

Type-I multiferroics contain those materials in which the source of magnetism and ferroelectricity are different and independent of each other. So, the coupling between these is very weak. In these materials, ferroelectricity appears at higher temperatures as compared to magnetism, and spontaneous polarization P is quite large. Examples are BiFeO_3 ($T_C = 1100 \text{ K}$, $T_N = 643 \text{ K}$, $P = 90 \mu\text{C}/\text{cm}^2$) and YMnO_3 ($T_C = 914 \text{ K}$, $T_N = 76 \text{ K}$, $P = 690 \mu\text{C}/\text{cm}^2$). There is a different mechanism of ferroelectricity in Type-I multiferroics are, explained below:

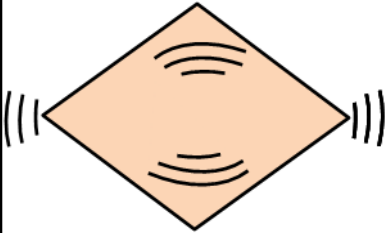
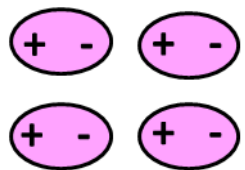
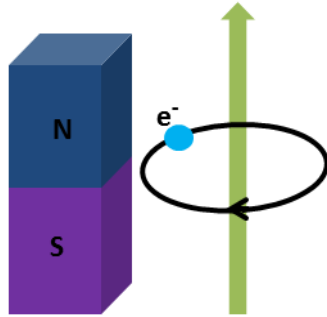
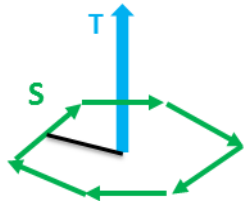
Space \ Time	Invariant	Change
Invariant	<p>Ferroelastic</p> 	<p>Ferroelectric</p> 
Change	<p>Ferromagnetic</p> 	<p>Ferrotoroidic</p> 

Fig. 1.8: Classification of ferroic orders with symmetry [Van Aken *et al.* 2007].

(a) Ferroelectricity due to lone pairs

The compounds such as BiFeO_3 , BiMnO_3 , and PbVO_3 have $6s$ electrons in the outer shell, and two electrons out of them don't take part in the chemical bonding; these are lone pairs or

dangling bonds. They have high polarizability. The ferroelectricity originated in these compounds by mixing p -orbitals with the lone pairs, as shown in Fig.1.9 (a) [Khomskii *et al.* 2009].

(b) Ferroelectricity due to charge ordering

The transition metal ion with different valance states leads to inequivalent bonds, which causes ferroelectricity, as shown in Fig.1.9 (b).

(c) Geometric ferroelectricity

In the compounds like YMnO_3 , ferroelectricity is caused due to tilting of MnO_5 polyhedra, and O^{2-} ions provide the closer packing while Mn^{3+} remains at the center. Due to polyhedral tilting, Y-O bonds form dipoles, as shown in Fig.1.9 (c).

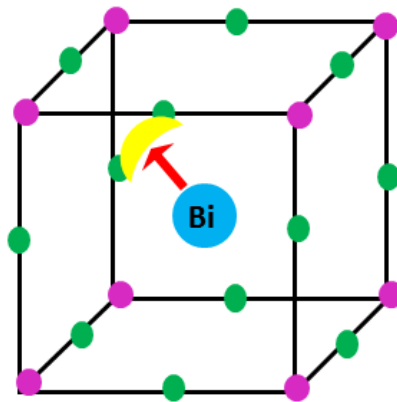


Fig. 1.9: (a) In BiFeO_3 , (yellow) lobes of O^{2-} ions and Bi^{3+} (blue) ion contribute to the polarization shown by the red arrow.

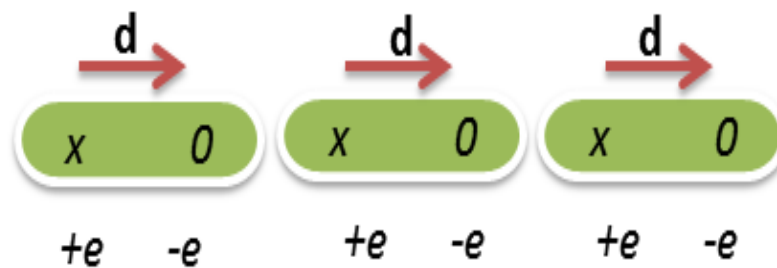


Fig. 1.9: (b) Ferroelectricity due to inequivalent bonds.

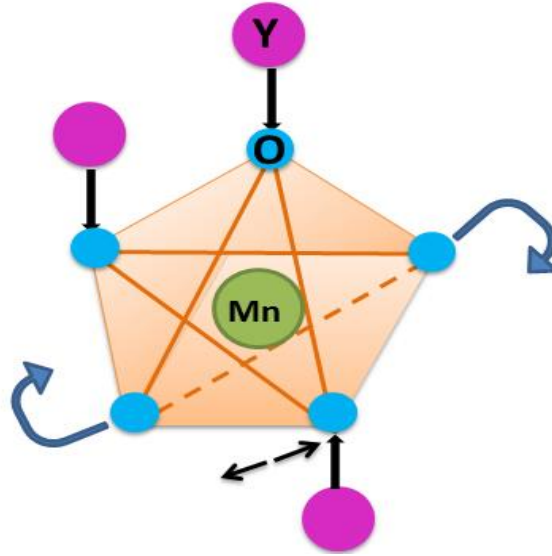


Fig. 1.9: (c) Ferroelectricity due to geometry.

1.4 Bismuth Ferrite (BiFeO₃)

BiFeO₃ (BFO) was discovered in the late fifties, but it was initially not produced in single-phase polycrystalline. Later in 1967, Achenbach prepared a single-phase BFO. Kubel and Schmid 1990 investigated the mono-domain single-phase by XRD. Although BFO showed simultaneous antiferromagnetic and ferroelectric properties but its polarization was observed to be very low, 6.1 $\mu\text{C}/\text{cm}^2$. For a very long time, the physical and structural properties of BFO were a source of controversy, so it did not find important for practical applications. Later in 2003, Wang *et al.* observed room temperature spontaneous electric polarization; it was unusually high ($\sim 50\text{-}60 \mu\text{C}/\text{cm}^2$) in BFO thin films, renewed the interest in these materials. Later in 2003, Neaton *et al.* reported the spontaneous polarization for BFO was observed at $\sim 90\text{-}100 \mu\text{C}/\text{cm}^2$.

1.4.1 Structure of BiFeO₃

BFO has rhombohedrally distorted perovskite structure with an $R3c$ space group at room temperature and atmospheric pressure, shown in Fig. 1.10. Unit cell parameters are $a_{\text{rh}} = 3.965 \text{ \AA}$ and $\alpha_{\text{rh}} = 89.3\text{-}89.4^\circ$. According to symmetry of BFO unit cell, the lattice parameters are $a_{\text{hex}} =$

$b_{\text{hex}} = 5.58 \text{ \AA}$ and $c_{\text{hex}} = 13.90 \text{ \AA}$. The Goldschmidt tolerance factor (t) = 0.88, which results in severe oxygen octahedra buckling due to the smaller size of cations at the A-site; empty space causes the octahedra tilting of $\sim 11\text{-}14^\circ$ around the polar axis [111] that deviates the Fe-O-Fe angle (θ) value of $154\text{-}156^\circ$ from 180° . [Catalan *et al.* 2009; Yang *et al.* 2012]. $R3c$ space group goes through two distinct phase transitions (a) paraelectric transition cubic phase ($\text{Pm}\bar{3}\text{m}$) with ferroelectric Curie temperature (T_C) of 1100 K, and (b) magnetic transition from a G-type antiferromagnetic state to a paramagnetic state at Neel temperature (T_N) of 643 K.

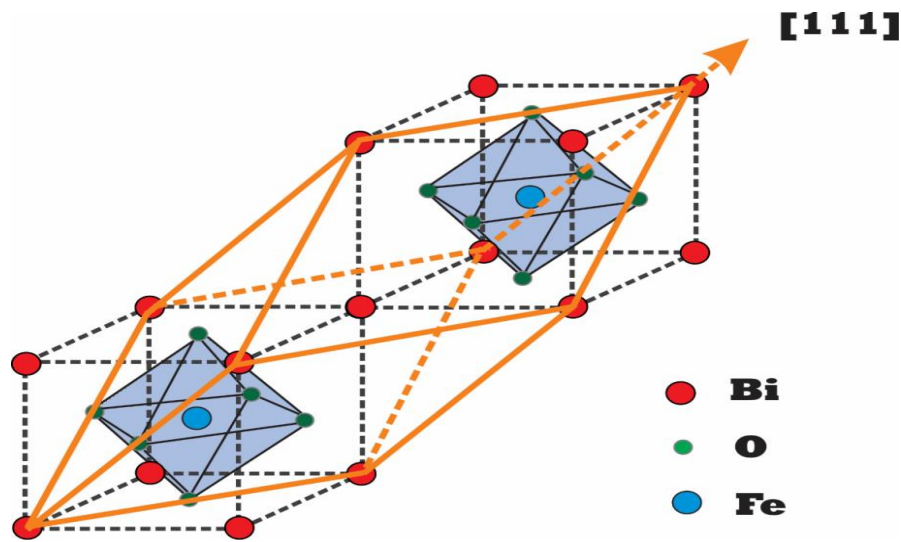


Fig. 1.10: Simplified crystal structure of BiFeO₃ [Gómez *et al.* 2016]

In certain cases, it has been found that the grain sizes below 30 nm change rhombohedral to cubic symmetry [Selbach *et al.* 2007]. In epitaxial thin films of BFO suggests rhombohedral, tetragonal, and monoclinic phases [Béa *et al.* 2006; Wang *et al.* 2003]. Wang *et al.* 2013 have reported that space group $P1$ could be more appropriate than polar space group $R3c$ to describe the structure of α -BiFeO₃ at room temperature. In BFO, ferromagnetism is due to a partially filled d^n orbital (Fe^{3+} ions), while ferroelectricity is due to the vacant d^0 orbital (stereochemically active lone pair orbital of $6s^2$ of Bi^{3+} ion). BiFeO₃ is a G-type anti-ferromagnet that represents a spin canting which results in a weak magnetic moment in the unit cell according to

Dzyaloshinskii-Moriya interaction. The net magnetic moment exhibits a long-range superstructure consisting of a spin cycloid with a 64 nm wavelength that is incommensurable with the crystallographic structure [Lebeugle *et al.*; Sosnowska *et al.*]. This results in zero magnetic moments, which prevents the magnetoelectric effect in the materials that can be recovered by the frustration of the spin cycloid using different methods.

1.4.2 Phase transitions in BFO

Fig. 1.11 shows the phase diagram of BFO. At temperatures around 370 °C, a second-order phase transition occurs from an anti-ferromagnetic to paramagnetic structure that is allied with anomalous lattice expansion [Selbach *et al.* 2008]. At temperature ~825 °C a first-order transition occurs from the paramagnetic α -BiFeO₃ phase to the high-temperature phase β -BiFeO₃ due to an abrupt decrement of the unit cell volume as well as change in atomic positions [Lu *et al.* 2011; Polomska *et al.* 1974; Palai *et al.* 2008]. The authors [Catalan *et al.* 2009; Selbach *et al.* 2008; Polomska *et al.* 1974] have reported centrosymmetry of the β -BiFeO₃ phase, and a phase transition occurs from the ferroelectric to paraelectric at temperature 825 °C. The symmetry of β -BiFeO₃ is controversial observed by many authors and reported as monoclinic symmetry (P21/m) [Hamout *et al.* 2008] with a monoclinic angle value of 90.01°; Orthorhombic phase with some coexistence of rhombohedral domains [Palai *et al.* 2008]; Rhombohedral R(-3)c [Selbach *et al.* 2008]. With the help of neutron diffraction, Arnold *et al.* [Arnold *et al.* 2009] have found that β -phase symmetry is orthorhombic. At higher temperature, ~ 933 °C, a second-order phase transition from β to γ phase of BiFeO₃ is reported, which has cubic symmetry belonging to the space group Pm(-3)m. At the temperature at which β to γ phase transition BiFeO₃ occurs, a sharp decrement of the band-gap towards zero indicates the transition from an electric insulator to metallic behavior [Palai *et al.* 2008].

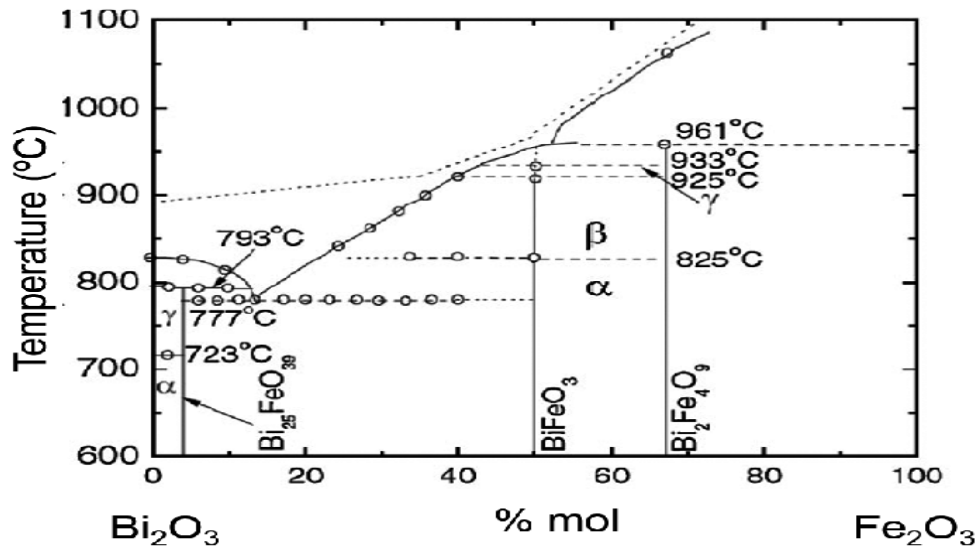


Fig. 1.11: Phase diagram of BFO [Palai *et al.* 2008]

1.4.3 Band structure of BFO

Bilc *et al.* in 2008, theoretically have calculated the highest direct band gap for BiFeO₃, the reported value is found to be 3.6 eV. However, the experimental value of the direct band gap is reported in the range of 2.6 to 3.0 eV. The band gap depends highly on the microstructure and the processing conditions, particle size, microstrain [Mocherla *et al.* 2013], and oxygen vacancy for nano-structures [Wang *et al.* 2020].

1.4.4 Applications and Limitations of BFO

- BFO as multiferroics has huge applications in storage devices like RAM and FERAM due to the high value of polarization. It is also used in piezoelectric actuators due to the significant value of d_{33} , spintronics-based devices, and energy harvesting due to photocatalytic properties. BFO can generate terahertz radiations, which can be used where leakage current is a huge problem.

- Synthesis of single-phase BFO is still difficult. It is always formed with smaller impurity phases like $\text{Bi}_{25}\text{FeO}_{39}$ (or $\text{Bi}_{25}\text{FeO}_{40}$) $\text{Bi}_2\text{Fe}_4\text{O}_9$.
- The volatile nature of Bi and hopping of $\text{Fe}^{3+} \leftrightarrow \text{Fe}^{2+}$ oxidation in BFO leads to non-stoichiometry by creating oxygen vacancies, which in turn enhances the leakage current. So, saturated ferroelectric hysteresis loops cannot obtain, as shown in Fig. 1.12.
- The difference between T_C and T_N is large (~ 460 K).
- RT electric field-induced decomposition into Fe_3O_4 .

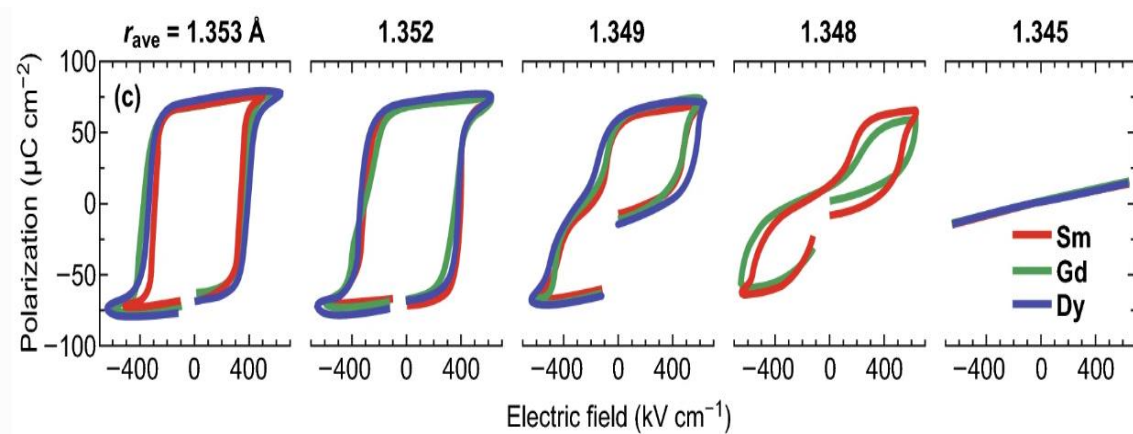


Fig. 1.12: Ferroelectric hysteresis loop of BFO [Palai *et al.* 2008]

1.5 Problem statement

It is believed that in case of perovskites, B-site substitution controls the dielectric properties and conductivity of the material. Moreover, A-site substitution also alters the bonding strength of B-O bond due to the competency between B-O and A-O bond. The aliovalent alters the band width which in turn modifies the tolerance factor. Over the past few years, many substitutions on A, B, and A-B both sites of BFO have been carried out to improve the magnetic and ferroelectric properties. Thus, different substitutions open opportunities for the development of new multiferroic materials for applications. It has also been noticed that A-site doping in perovskite-based compounds is more effective. Further, effect of A-site and B-site substitution on dielectric

anomalies specifically Polomska transition and its effect on the properties are discussed. Further, effect of substitution on leakage current is also explored.

1.6 Organization of the thesis

The thesis has been divided into 7 chapters

Chapter 1: A brief description of multiferroics, their classification, properties and applications in different fields, problem statement and organization of the thesis.

Chapter 2: Literature review based on the improvement in electromagnetic properties of bismuth ferrite.

Chapter 3: Different experimental techniques and instruments used in this research work.

Chapter 4: Discuss about the effect of Gd doping on the dielectric and magnetic properties of BSFO based multiferroic system.

Chapter 5: Explain about the influence on properties of $\text{Bi}_{0.9}\text{Sm}_{0.1}\text{FeO}_3$ multiferroic system with Mg substitution at Fe-site.

Chapter 6: Describe about the microstructural, dielectric and conduction mechanism of $1-x(\text{Bi}_{0.9}\text{Sm}_{0.1}\text{FeO}_3) - x(\text{BaZr}_{0.15}\text{Ti}_{0.85}\text{O}_3)$ ($x = 0.0, 0.1, 0.15, 0.2, 0.25, 0.5$) solid solution ceramics.

Chapter 7: Covers the concluding remarks and the future scope of this work.

Finally, towards the end of the thesis complete list of references has been included and at last concise list of publications and conferences related to present research work has been attached.